

Semi-interpenetrating network based on cross-linked poly(vinyl alcohol) and poly(styrene sulfonic acid-*co*-maleic anhydride) as proton exchange fuel cell membranes

C.W. Lin^{a,*}, Y.F. Huang^a, A.M. Kannan^b

^a Department of Chemical Engineering, National Yunlin University of Science and Technology, Yunlin, Taiwan

^b Department of Electronic Systems, Arizona State University at the Polytechnic Campus, Mesa, AZ 85212, United States

Received 29 August 2006; received in revised form 24 October 2006; accepted 25 October 2006

Available online 5 December 2006

Abstract

A series of promising proton conducting membranes have been synthesized by using poly(vinyl alcohol), with sulfosuccinic acid (SSA) as a cross-linking agent and poly(styrene sulfonic acid-*co*-maleic acid) (PSSA-MA) as proton source, which form a semi-interpenetrating network (semi-IPN) PVA/SSA/PSSA-MA membrane. A bridge of SSA between PVA molecules not only reinforces the network but also provides extra proton conducting paths. PSSA-MA chains trapped in the network were the major sources of protons in the membrane. FT-IR spectra confirmed the success of the cross-linking reaction and molecular interactions between PVA and PSSA-MA. Associated characteristics of a proton conducting membrane including ion-exchange capacity (IEC), proton conductivity and water uptake were investigated. The measured IECs of the membranes increased with increase of PSSA-MA content varying from 20 to 80% and correlated well with the measured uptake water and proton conductivity. The semi-IPN membranes with PSSA-MA over 60% exhibited a higher proton conductivity than Nafion-115 and also a reasonable level of water uptake. Fuel cell performance of membrane electrode assemblies (MEA) was evaluated at various temperatures with H₂/air as well as H₂/O₂ gases under ambient pressure. A power density of 0.7 W cm⁻² was obtained for the MEA using PVA/SSA20/PSSA-MA80 membrane using H₂/O₂ at 50 °C.

© 2006 Elsevier B.V. All rights reserved.

Keywords: Proton conducting membrane; Semi-interpenetrating network; Poly(vinyl alcohol); Poly(styrene sulfonic acid-*co*-maleic acid); Membrane electrode assembly; Fuel cells

1. Introduction

The proton exchange membrane fuel cell (PEMFC) is one of the most attractive power sources for a variety of applications by virtue of its high efficiency and environmentally friendly nature [1–3]. A PEMFC requires a membrane to separate the chemical reaction at the anode from that at the cathode both chemically and electronically. A successful fuel cell membrane must allow protons to move freely. This requirement has led to great interest in cation exchange membranes. To date, perfluorinated sulfonic acid membrane (Nafion, manufactured by DuPont) has been the most commonly used membrane in a low temperature hydrogen/oxygen fuel cell (H₂/O₂FC)

because it combines required chemical, electrochemical and mechanical stabilities with high proton conductivity. However, due to a high production cost, low operating temperature and significant fuel cross-over, considerable efforts have gone into searching for alternative proton exchange membranes for both the H₂/O₂FC and the direct methanol fuel cell (DMFC) [4,5].

Among a variety of different approaches to synthesizing new electrolyte membranes, acid-base polymer blends have become a favorite approach to the design of improved PEM materials due to the interaction (ionically cross-linked) between polymers and these interactions can reduce significantly the swelling and the methanol permeability of membranes [6,7]. A series of different polymer blends, such as sulfonated poly(ether ether ketone) (SPEEK) blended with poly(ether imide) (PEI), poly(amide imide) (PAI), and poly(benzimidazole) (PBI), have been reported in the literature [8–10].

* Corresponding author. Tel.: +886 5 534 2601x4613; fax: +886 5 531 2071.
E-mail address: lincw@yuntech.edu.tw (C.W. Lin).

Due to its high selectivity of water to alcohols, poly(vinyl alcohol) (PVA) membranes have been used in alcohol dehydration to break the alcohol–water azeotrope [11–14]. Taking advantage of this high selectivity, Pivovar et al. [15] explored the potentiality of PVA as proton exchange membrane in DMFC based on proton conductivity and methanol permeability experiments. The authors reported that the PVA membranes employed in a pervaporation process were much better methanol barriers than Nafion. Later, Li and Wang [16,17] prepared proton-conducting membranes based on PVA with embedded phosphotungstic acid (PWA) and found that water uptake, proton conductivity and methanol permeability were increased with PWA content. In order to improve the durability and thermal stability of a PVA/PWA membrane, SiO₂ was incorporated [18]. PVA blends with poly(styrene sulfonic acid-*co*-maleic acid) (PSSA-MA), poly(2-acrylamido-2-methyl-1-propanesulfonic acid) (PAMPS), and sulfonated phenolic resin (S-Ph) [19–22] have also been investigated. Recently, Rhim and coworkers [23,24] have prepared and characterized cross-linked PVA membranes containing sulfonic acid group for DMFC applications.

Most of the previous studies on PVA-based membranes dealt with preparation and characterizing them towards transport properties but none of them focused on fabricating membrane electrode assemblies (MEA) for fuel cell tests. To our knowledge, this paper is the first one to evaluate the potential of PVA-based membranes for H₂/O₂FC applications. This paper describes the preparation of PVA-based semi-IPN membranes and looks at the influences of the penetrating poly(styrene sulfonic acid-*co*-maleic acid) with the membrane properties such as water uptake, ion-exchange capacity (IEC), proton conductivity. Furthermore, membranes with good physicochemical properties were fabricated into membrane electrode assemblies for fuel cell testing with H₂/air as well as H₂/O₂ at various temperatures.

2. Experimental

2.1. Materials

Poly(vinyl alcohol) (Aldrich, average molecular weight: 89,000–98,000 g mol⁻¹; degree of hydrolysis: 99%; Fluka, average MW: 130,000 and 195,000 g mol⁻¹; degree of hydrolysis: 88% and 99%, respectively), sulfosuccinic acid, as a cross-linking agent (SSA, 70 wt.% solution in water, Aldrich) and poly(styrene sulfonic acid-*co*-maleic acid) (sodium salt, the ratio of styrene sulfonic acid to maleic acid is 3/1, average MW = 20,000 g mol⁻¹; Aldrich) were used to prepare proton conducting membranes. All chemicals were used without further purification. Platinized carbon (46.4% Pt on carbon—TEC1050E) from Tanaka Kikinzoku Kogyo KK, Japan was used as electrocatalyst for fabricating catalyst coated membranes.

2.2. Preparation of membrane

Preparation steps of a semi-IPN membrane are given in Fig. 1 schematically. In brief, PVA powder was dissolved in de-ionized

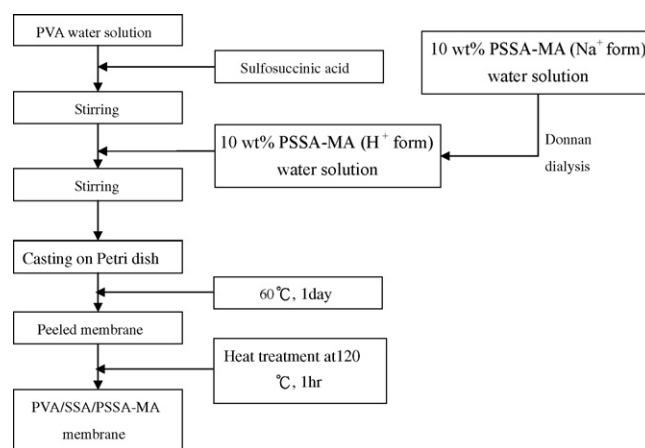


Fig. 1. Schematic illustration of preparation procedures of PVA/SSA/PSSA-MA semi-IPN membrane.

water at 60 °C with continuous stirring. The PVA solution was mixed with a given amount of SSA of the desired concentration and the mixture was stirred continuously at 60 °C until a homogeneous solution was obtained. To facilitate interaction of PSSA-MA with PVA, PSSA-MA was first dissolved in de-ionized water (10 wt.% solution) and then was transformed from Na⁺ to H⁺ form via Donnan dialysis (two-compartment cell, equipped with Nafion-115 and 1 M HCl).

The selected amount of PSSA-MA was added to the PVA/SSA solution and was stirred at 60 °C until homogeneous solution was obtained. The membranes were cast by pouring the solutions onto Petri dishes and evaporating the water at 60 °C for 1 day. Membranes were peeled off from the dish and annealed at 120 °C for 1 h. The amount (%) of SSA and PSSA-MA were determined by the weight of PVA. After cooling down to room temperature suddenly, the resultant membranes were stored in de-ionized water. FT-IR/ATR was used to identify the success of cross-linking reactions and the associated molecular interactions in membrane structure.

2.3. Characterization of proton conductivity membrane

Infrared spectra were recorded in the transmittance mode on a Perkin-Elmer FT-IR spectrometer in the range of wave numbers 600–4000 cm⁻¹. The resolution and number of scans in all spectra were 4 and 16 cm⁻¹, respectively.

Proton conductivity measurements were carried out at ambient temperature after equilibrating the membranes in de-ionized water for 1 day. The proton conductivity cell composed of two stainless steel electrodes of 9.5 mm diameter. The membrane sample was sandwiched between the stainless steel electrodes. AC impedance spectra of the membranes were recorded from 200,000 to 100 Hz with an amplitude of 5 mV by using an Auto-lab PGSTST 30 instrument. The resistance value associated with the membrane proton conductivity was determined from the high frequency intercept of the impedance with the real axis. The proton conductivity was calculated according to

$$\sigma = \frac{L}{RA}$$

where σ , L , R , and A denote the proton conductivity, thickness (which was measured using micrometer), the measured resistance, and the cross-sectional area of the membranes perpendicular to current flow, respectively.

Ion-exchange capacity (IEC) values of the proton conducting membranes were determined by the titration method. Each hybrid membrane was soaked in 1 M sodium chloride aqueous solution for 1 day to exchange protons with sodium ions. The ion-exchanged solution was then titrated with 0.005 M sodium hydroxide solution. The IEC value was calculated using the following equation:

$$\text{IEC} = \frac{M_{i, \text{NaOH}} - M_{f, \text{NaOH}}}{W_{\text{dry}}} = \frac{H^+ (\text{mmol})}{W_{\text{dry}}}$$

where $M_{i, \text{NaOH}}$ is the initial mmol of NaOH of titration and $M_{f, \text{NaOH}}$ is the mmol (mequiv.) of NaOH after equilibrium, H^+ is the molar number of proton sites presented in the membrane, and W_{dry} is the weight of dry membrane.

The water uptake values of the membranes were determined by measuring the change in the weight before and after the hydration. Pre-dried membranes were immersed in de-ionized water for 24 h, and then surface-attached water on the membranes was removed with filter paper. After that, the wet membrane weight (W_{wet}) was determined as quickly as possible. Weight of dry membrane (W_{dry}) was determined after completely drying in vacuum at 60 °C for 24 h. The water uptake (%) values of the membrane were calculated by using the following equation:

$$\text{water uptake} = \frac{W_{\text{wet}} - W_{\text{dry}}}{W_{\text{dry}}} \times 100$$

2.4. Preparation of MEAs and evaluation of single cell performance

Catalyst coated membranes (CCM) were fabricated using Pt/C catalyst slurry in isopropanol using the micro-spray method. In order to extend the reaction zone of the catalyst layer, 5% Nafion solution (30 wt.% to Pt catalyst) was added to the catalyst slurry. The catalyst loadings on the anode and cathode sides were about 0.5 mg Pt cm⁻², respectively. Gas diffusion layer (GDL) was prepared with teflonized non-woven 7 mil carbon paper (P50T, Ballard Applied Materials) substrate as follows. A slurry of graphitized carbon black grade PUREBLACK 205-

110 carbon (Superior Graphite Co., Chicago, IL, USA) with PTFE (TE 3859 Teflon suspension from Dupont) dispersion in a mixture of isopropanol and de-ionized water (80:20 volume ratio) was prepared by ultrasonication for 20 min followed by a magnetic stirring for about 2 h. The micro-porous layer was fabricated by applying the slurry on the carbon paper by micro-spraying method. Subsequently, carbon paper with micro porous layer was heat treated by sintering at 350 °C under vacuum for about an hour. The carbon loading for the micro-porous layer was approximately 3.5 mg cm⁻² and the PTFE content was 30 wt.%.

MEAs were assembled by just sandwiching the catalyst coated membrane with the GDLs inside the test cell (Fuel Cell Technologies). Gas sealing was carried out using silicone coated fabric materials (Performance Plastics, CF1007) at a uniform torque of 40 lb in [25]. The MEAs were evaluated by a linear sweep voltammetry (LSV) and a cyclic voltammetry (CV) at various temperatures at 100% RH using Autolab Potentiostat/Galvanostat PG50 for measuring hydrogen gas cross-over of the membranes and electrochemically active surface area (ECA) of the catalyst, respectively. The test cell was equilibrated for about 2 h with humidified hydrogen and nitrogen gases (100 SCCM) before the voltage scanning for LSV and CV measurements. Single cell fuel cell performance was evaluated using Greenlight G40 (Hydrogenics Test Systems, Burnaby, Canada) Test Station at various temperatures using H₂/air as well as H₂/O₂ under ambient pressure by galvanostatic polarization. The relative humidity of the reactant gases (H₂, air, N₂ and O₂) were maintained at 100% by controlling the humidity bottle temperatures.

3. Result and discussion

3.1. Molecular interactions by FT-IR

The scheme of cross-linking reaction between PVA and SSA is shown in Fig. 2. The bridge between PVA molecular chains through SSA provided not only required resistance to water dissolution but also proper mechanical strength of membrane. Besides, SSA also plays a role of one of proton carrier through its pendant sulfonic acid group. Fig. 3 shows the FT-IR spectra for pristine PVA, PVA/SSA, and PVA/SSA/PSSA-MA membranes. As seen from the figure, the PVA/SSA membrane shows a characteristic absorption band at 1714 cm⁻¹ (C=O), and C–O stretch mode of ester group at 1206 cm⁻¹ due to the formation

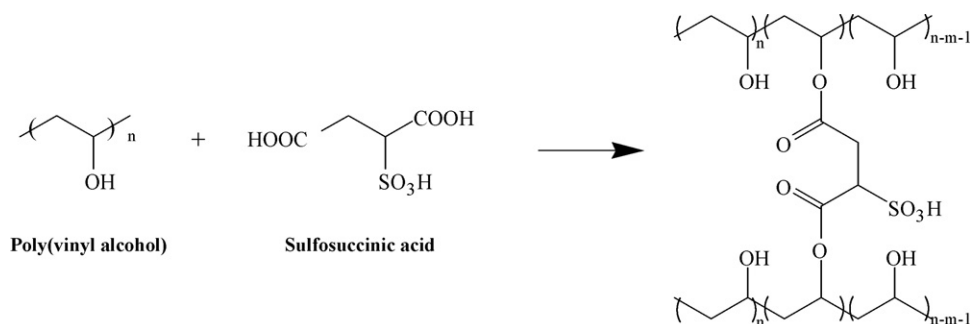


Fig. 2. The scheme of cross-linking reaction between PVA and SSA.

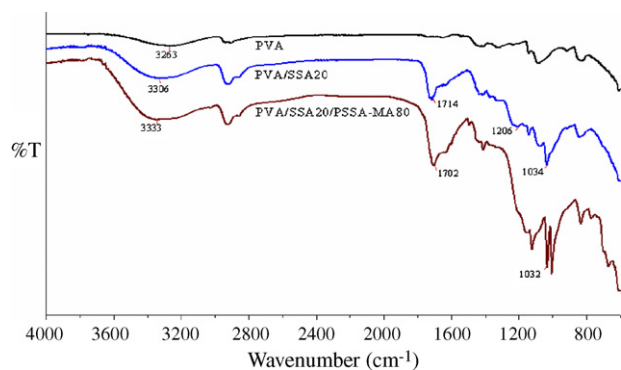


Fig. 3. FT-IR Spectra of PVA, PVA/SSA and PVA/SSA/PSSA-MA membranes.

of ester bonds (C–O–C) between the alcohol group of PVA and carboxyl group of PSSA-MA. Furthermore, the absorption band observed at 1034 cm^{-1} is assigned to $-\text{SO}_3$ group of SSA. For PVA/SSA/PSSA-MA membrane, the absorption bands assigned to $-\text{OH}$ stretching vibration were observed in the range of $3200\text{--}3600\text{ cm}^{-1}$. In pristine PVA, intra-molecular and inter-molecular hydrogen bonds are expected to occur among PVA chain due to high hydrophilic force [26]. The $-\text{OH}$ group of pristine PVA (3263 cm^{-1}) shifts progressively to higher wavelength region during cross-linking (3306 cm^{-1}) and incorporation of PSSA-MA (3333 cm^{-1}). This indicates that the cross-linking reaction occurred between PVA and SSA by creating new covalent bonds and reducing hydrogen bonds between PVA chains. After adding PSSA-MA, the strong interaction between hydroxyl groups on PVA and sulfonic acid or carboxyl acid groups on PSSA-MA intensively reduce the hydrogen bonds formation between PVA chains, leading to a more effective mixing of all constituents. The resulting semi-IPN molecular structure is illustrated schematically in Fig. 4. Although PVA manifests itself as hydrophobic nature in main chain and does not have fixed charges, $-\text{SO}_3\text{H}$ from both SSA and PSSA-MA as well as $-\text{COOH}$ from PSSA-MA impart hydrophilicity and ionic groups of the semi-IPN structure.

3.2. Membrane characterization by IEC, water uptake and proton conductivity

According to our preliminary studies, an optimum amount of 20 wt.% of SSA cross-linking agent was determined to be 20 wt.% in terms of swelling level and mechanical property. In

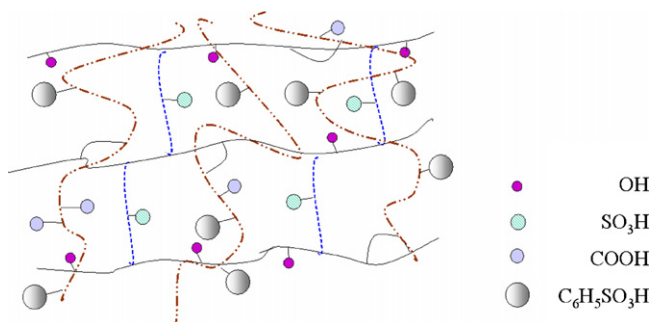


Fig. 4. The semi-IPN structural scheme of PVA/SSA/PSSA-MA membrane.

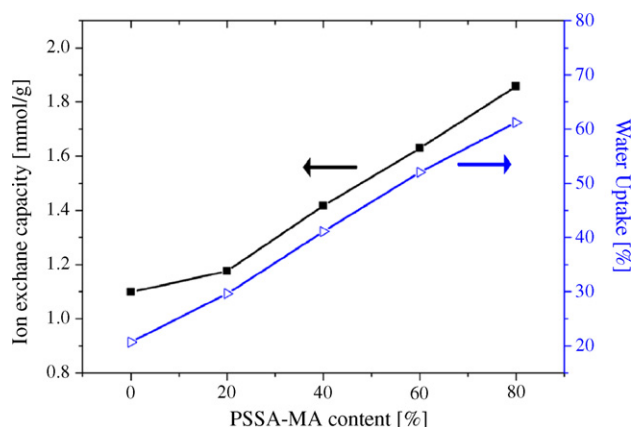


Fig. 5. IEC, water uptake of semi-IPN membranes based on PVA/SSA20 with different amounts of PSSA-MA trapped in the network.

the present study, a fixed amount of SSA 20 wt.% was used to construct the PVA network. As seen from Fig. 5, due to the increase of sulfonic acid and maleic acid on PSSA-MA, the measured IEC values of the membranes increase from 1.1 to 1.86 mmol g^{-1} with increase of PSSA-MA content varying from 20 to 80%. Water uptake plays a critical role in proton conduction as water is the major carrier of protons. However, excess swelling in water reduces membrane's mechanical strength. In addition to IEC values, Fig. 5 also shows the water uptake as a function of PSSA-MA content. The water uptake values increase from 20 to 60% when PSSA-MA content increased from 0 to 80 wt.%. Obviously, the increase in water uptake is due to the increasing number of hydrophilic groups in PSSA-MA.

Fig. 6(a) presents the proton conductivity of PVA/SSA20/PSSA-MA membranes as a function of PSSA-MA content at room temperature. As expected, the proton conductivity values increased with PSSA-MA content. When PSSA-MA content is up to 80%, the proton conductivity reached to about $2.59 \times 10^{-2}\text{ S cm}^{-1}$, comparable to that of Nafion-112 [27]. It is well known that both water uptake and IEC have profound effects on membrane conductivity. Higher water uptake promotes the transportation of proton more effectively and higher IEC decreases the distance between anionic groups leading to faster proton conduction. All the measured important properties related to proton exchange membrane are summarized in Table 1. It can be concluded that a higher PSSA-MA content plays a major role in controlling the proton conduction due to the increase of sulfonic acid and carboxylic acid groups in the membrane. However, higher amount of PSSA-MA also lead to excessive swelling in water causing undesired mechanical instability of the membranes. The membrane of PVA/SSA20/PSSA-MA80 therefore manifested its superior characteristic in practical fuel cell applications.

3.3. Effect of temperature on proton conductivity

Proton conductivity data obtained at various temperatures are summarized in Table 2 along with that for Nafion-112 membrane. The temperature dependence of proton conductivity for several compositions of semi-IPN membrane samples are plot-

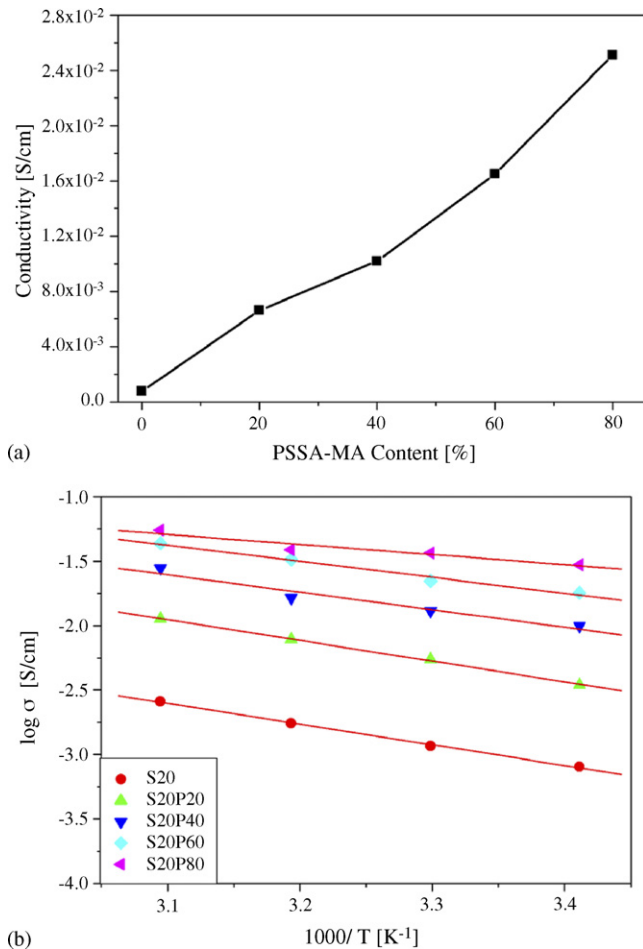


Fig. 6. (a) The proton conductivity of PVA/SSA20/PSSA-MA membranes as a function of PSSA-MA amount and (b) temperature dependence of proton conductivity by plotting $\log \sigma$ vs. $1/T$.

ted in Fig. 6(b) along with that for Nafion-115 membrane. Evidently, the change of proton conductivity with temperature follows the Arrhenius relationship in the experimental temperature range of 20–50 °C.

$$\sigma = \sigma_0 \exp\left(\frac{-E_{a,\text{cond}}}{kT}\right)$$

where k is the Boltzman constant and $E_{a,\text{cond}}$ is the activation energy of proton conduction, which can be derived from the slope of $\log \sigma$ versus $1/T$ plots. All the membranes exhibited positive temperature-conductivity dependencies. The $E_{a,\text{cond}}$ for proton conduction decreased with an introduction of PSSA-MA into cross-linked PVA network. This can be explained by the increase of free water contained in the membranes with higher loading of hydrophilic ionomer. According to vehicle mechanism [15], the free water can act as a proton-carrying medium. The activation energy values range from 15 to 30 kJ mol⁻¹, which is higher than that for Nafion membrane (9.9 kJ mol⁻¹ for Nafion). It can be deduced that both the vehicle mechanism and the Grotthuss mechanism are responsible for the proton conduction of the semi-IPN membranes and it is expected that the semi-IPN membranes would be more favorable in the higher temperature.

3.4. MEA and single cell performance

Fig. 7(a) shows the LSV data for an MEA containing a membrane PVA/SSA20/PSSA-MA80 (MW: 89,000–98,000 g mol⁻¹, thickness: 80 μm) and Pt/C at various temperatures at 100% RH. As seen from the data, the hydrogen cross-over current density of about 6–8 mA cm⁻² were observed in the temperature range of 25–60 °C. It is interesting to see that the cross-over current density did not increase significantly with increasing temperature. Fig. 7(b) shows the cyclic voltammetry

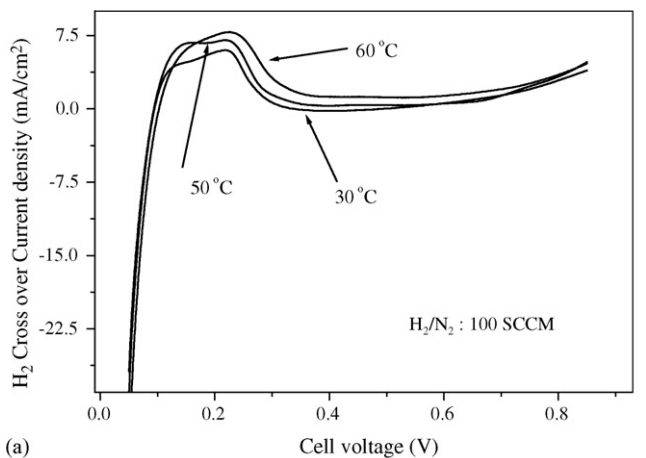
Table 1
Measured IECs, water uptakes, and proton conductivities of various PVA/SSA20/PSSA-MA and Nafion membranes

Membrane	Measured IEC (mmol g ⁻¹)	Water uptake (wt.%)	Proton conductivity (S cm ⁻¹)
PVA/SSA20	1.10	20.2	7.64×10^{-4}
PVA/SSA20/PSSA-MA20	1.17	29.3	6.63×10^{-3}
PVA/SSA20/PSSA-MA40	1.42	40.4	1.02×10^{-2}
PVA/SSA20/PSSA-MA60	1.63	50.7	1.66×10^{-2}
PVA/SSA20/PSSA-MA80	1.86	62.9	2.51×10^{-2}
Nafion 112 ^a	0.91	30	6.00×10^{-2}

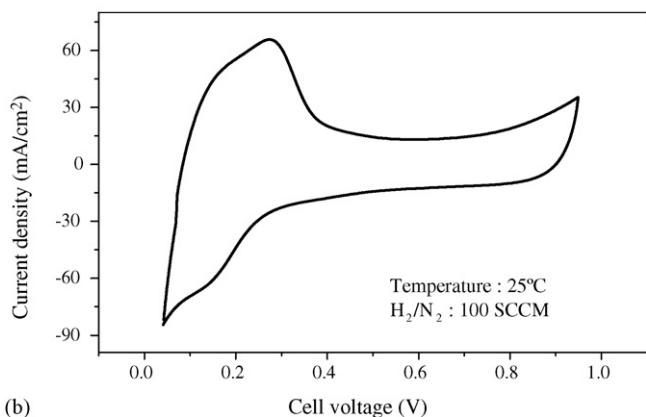
^a Data obtained from Ref. [27].

Table 2
Dependence of proton conductivity of PVA/SSA/PSSA-MA membranes as function of temperatures and activation energy calculated according to Arrhenius equation

Membrane	Proton conductivity (S cm ⁻¹)				Activation energy (kJ mol ⁻¹)
	20 °C	30 °C	40 °C	50 °C	
PVA/SSA20	8.04×10^{-4}	1.16×10^{-3}	1.75×10^{-3}	2.58×10^{-3}	30.76
PVA/SSA20/PSSA-MA20	3.46×10^{-3}	5.47×10^{-3}	7.82×10^{-2}	1.13×10^{-2}	30.77
PVA/SSA20/PSSA-MA40	9.94×10^{-3}	1.29×10^{-2}	1.63×10^{-2}	2.78×10^{-2}	25.99
PVA/SSA20/PSSA-MA60	1.79×10^{-2}	2.22×10^{-2}	3.25×10^{-2}	4.35×10^{-2}	23.86
PVA/SSA20/PSSA-MA80	2.96×10^{-2}	3.65×10^{-2}	3.88×10^{-2}	5.49×10^{-2}	14.98
Nafion	1.95×10^{-2}	2.33×10^{-2}	2.56×10^{-2}	2.87×10^{-2}	9.90



(a)



(b)

Fig. 7. (a) Linear sweep voltammetry (5 mV s^{-1} scan rate) and (b) cyclic voltammetry (50 mV s^{-1} scan rate) diagnostic test data for MEAs using membrane PVA/SSA20/PSS-MA80 (MW: 89,000–98,000 g mol^{-1} and thickness: $80 \mu\text{m}$) and Tanaka catalyst (Pt/C) with Hydrogen and nitrogen gases at 100% RH.

gram of an MEA fabricated by the CCM process containing a catalyst loading of $0.5 \text{ mg Pt cm}^{-2}$ on both anode and cathode, respectively for the membrane PVA/SSA20/PSS-MA80 at 25°C at 100% RH. The electrochemically active surface area calculated from the hydrogen desorption is about $45 \text{ m}^2 \text{ g}^{-1}$ Pt.

Fig. 8 shows fuel cell performance of an MEA using the semi-IPN membrane PVA/SSA20/PSS-MA80 (MW:

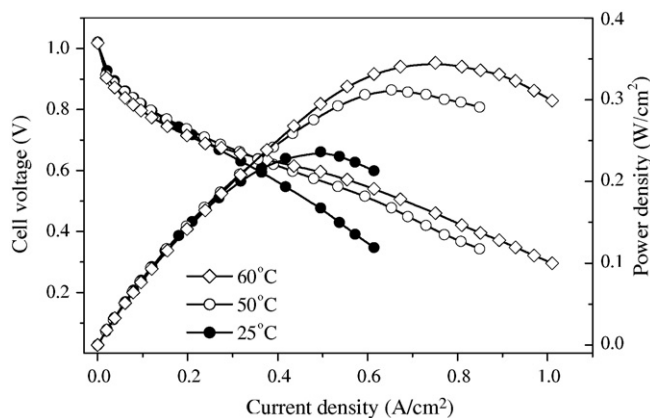


Fig. 8. Fuel cell performance of an MEA using the semi-IPN membrane PVA/SSA20/PSS-MA80 (MW: 89,000 g mol^{-1} and thickness: $80 \mu\text{m}$) at 25, 50, 60°C with hydrogen and oxygen at ambient pressure.

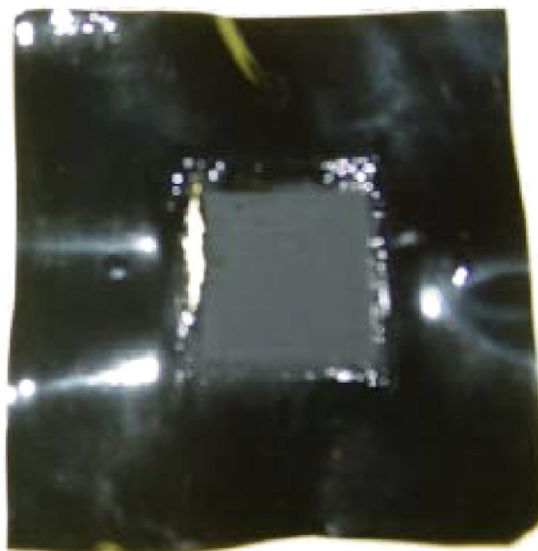


Fig. 9. Photograph of a catalyst coated membrane PVA/SSA20/PSS-MA80 (MW: 89,000–98,000 g mol^{-1} and thickness: $80 \mu\text{m}$) taken out from the FC test cell showing edge failure at edge after long operation time at 60°C .

89,000–98,000 g mol^{-1} , thickness: $80 \mu\text{m}$) at various temperatures (25 , 50 , and 60°C) with hydrogen and oxygen at ambient pressure. As can be seen, there is a consistent improvement in fuel cell performance as the cell temperature increases from 25 to 60°C . A power density value of 0.35 W cm^{-2} was obtained at 60°C using hydrogen/oxygen at 100% RH and ambient pressure. However, the MEA performance deteriorated with time (after 3 h) at an operating temperature of 60°C at a constant current density of 0.6 A cm^{-2} . An edge failure was noticed for the catalyst-coated membrane when the test cell was dismantled. A photograph of such a failed MEA is shown in Fig. 9. The edge failure is ascribed to the brittle nature of membrane with high degree of cross-linking, which is hard to compromise with the swelling behavior of membrane with a high hydrophilic functionality from PSSA-MA.

Fig. 10 shows the fuel cell performance of an MEA using the semi-IPN membrane PVA/SSA20/PSS-MA80 (MW:

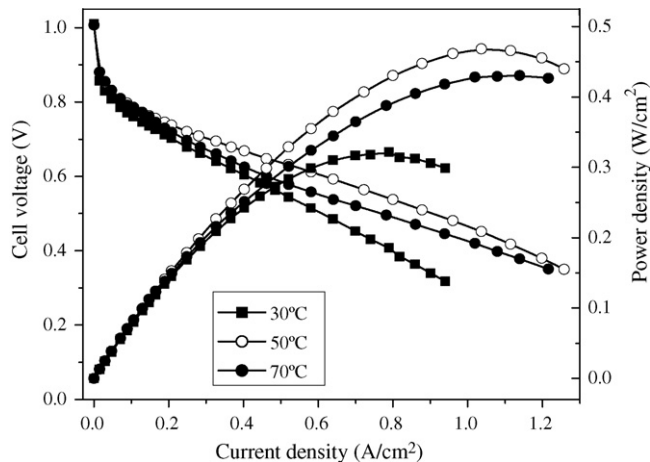


Fig. 10. Fuel cell performance of an MEA using the semi-IPN membrane PVA/SSA20/PSS-MA80 (MW: 130,000 g mol^{-1} and thickness: $50 \mu\text{m}$) at 30, 50, 70°C with hydrogen and oxygen at ambient pressure.

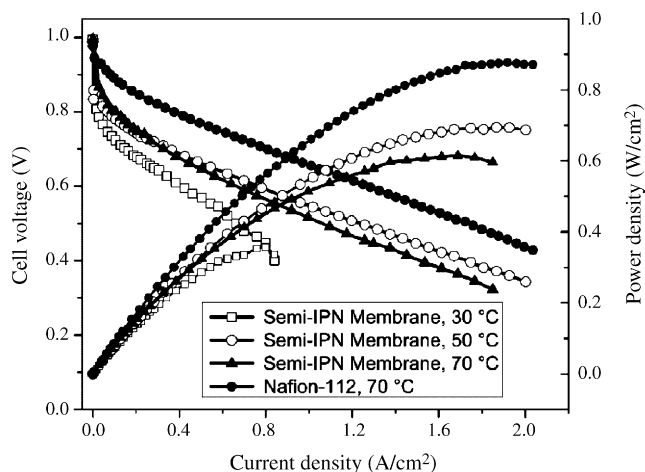


Fig. 11. Comparison of fuel cell performances of the MEAs using semi-IPN membrane PVA/SSA20/PSS-MA100 (MW: 130,000 g mol⁻¹ and thickness: 40 μm) at 30, 50, 70 °C and Nafion-112 at 70 °C with hydrogen and oxygen at ambient pressure.

130,000 g mol⁻¹, thickness: 50 μm) at 30, 50, 70 °C with hydrogen and oxygen at ambient pressure. A power density value of above 0.45 W cm⁻² was achieved at 50 °C at 100% RH. However, the performance of the MEA at 70 °C is lower than that at 50 °C. The lower performance at 70 °C could be due to the edge failure of the catalyst coated membrane, as noticed for the MEA with PVA/SSA20/PSS-MA80 (MW: 89,000–98,000 g mol⁻¹, thickness: 80 μm) membrane at 60 °C operation (Fig. 9). Fig. 11 compares fuel cell performance of the MEAs using the semi-IPN membrane PVA/SSA20/PSS-MA100 (MW: 130,000 g mol⁻¹, thickness: 40 μm) at 30, 50, and 70 °C with Nafion-112 based MEA at 70 °C. As can be seen, a power density of 0.7 W cm⁻² was obtained for the MEA using the semi-IPN membrane at 50 °C. The data also presents excellent mass transport characteristics of the MEAs at relatively high current density regions. As seen from the figure, the power density of semi-IPN membrane based MEA is only slightly lower than that of Nafion-112 under identical operating con-

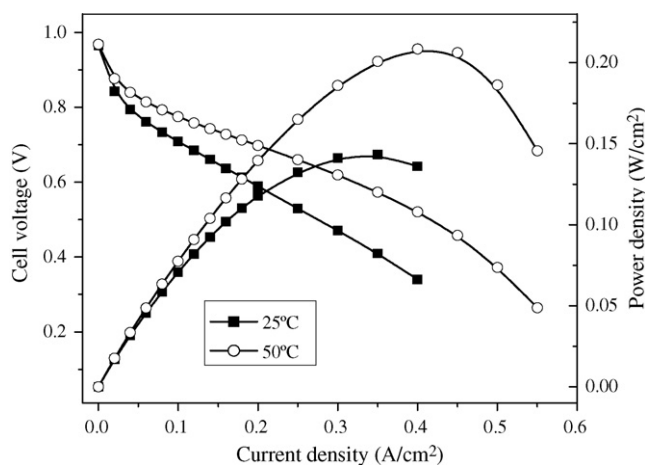


Fig. 12. Fuel cell performance of an MEA using the semi-IPN membrane PVA/SSA20/PSS-MA100 (MW: 195,000 g mol⁻¹ and thickness: 80 μm) at 25 and 50 °C with hydrogen and air at ambient pressure.

ditions. As observed with membrane PVA/SSA20/PSS-MA80 (MW: 130,000 g mol⁻¹, thickness: 50 μm)-based MEA at 70 °C (Fig. 10), this MEA also showed slightly lower performance at 70 °C compared to that at 50 °C. Taking advantage of higher degree of molecular chains entanglement, a higher molecular weight of PVA was employed for new sample here to improve the MEA's durability. The use of higher MW manifests an advantage of being able to accommodate higher amount of PSSA-MA without suffering excessive swelling. An MEA was fabricated with a membrane PVA/SSA20/PSSA-MA100 (MW: 195,000 g mol⁻¹, thickness: 80 μm) and the fuel cell performance was evaluated using hydrogen and air. Fig. 12 shows the fuel cell performance at 25 and 50 °C using hydrogen and air at 100% RH. A power density value of only about 200 mW cm⁻² was observed with hydrogen and air. The lower power density value could also be due to higher membrane thickness.

4. Conclusions

In this study, a series of semi-IPN proton conducting membranes have been prepared with a cross-linked PVA/SSA network and PSSA-MA. The completion of the cross-linking reaction and molecular interactions between PSSA-MA and PVA were confirmed by FT-IR spectra. The measured IECs of the membranes increased with increase of the PSSA-MA content varying from 20 to 80% and it correlated well with the water uptake and the proton conductivity. The semi-IPN membranes with PSSA-MA over 60% had higher proton conductivity than Nafion-115 and also a reasonable uptake water. Membrane-electrode assemblies were also evaluated in a direct hydrogen fuel cell using catalyst coated membranes. A power density of 0.35 W cm⁻² with hydrogen/oxygen at ambient pressure was obtained for an MEA using the semi-IPN membrane PVA/SSA20/PSSA-MA80 (MW: 89,000–98,000 g mol⁻¹) at 60 °C at 100% RH. Power density of 0.7 W cm⁻² with hydrogen/oxygen was obtained with a higher molecular weight (130,000 g mol⁻¹) membrane PVA/SSA20/PSSA-MA100 at 50 °C with excellent mass transport characteristics at relatively high current density regions.

Acknowledgements

The authors are grateful to the National Science Council of Taiwan (ROC) for the financial support of this work under the National Research Program for Nanoscience and Technology through Grant NSC95-2120-M-011-002. AMK acknowledges financial support from ASU.

References

- [1] J. Larminie, A. Dicks, *Fuel Cell Systems Explained*, Wiley, Great Britain, 2000.
- [2] P. Costamagna, S. Srinivasan, *J. Power Sources* 102 (2001) 242–252.
- [3] P. Costamagna, S. Srinivasan, *J. Power Sources* 102 (2001) 253–269.
- [4] O. Savadogo, *J. New Mat. Electrochem. Syst.* 1 (1998) 47–66.
- [5] O. Savadogo, *J. Power Sources* 127 (2004) 135–161.
- [6] M. Walker, K.-M. Baumgärtner, M. Kaiser, J. Kerres, A. Ullrich, E. Rächle, *J. Appl. Polym. Sci.* 74 (1999) 67–73.

- [7] J. Kerres, *J. Membr. Sci.* 185 (2001) 3–27.
- [8] J. Kerres, A. Ullrich, F. Meier, T. Häring, *Solid-State Ionics* 125 (1999) 243–249.
- [9] H.-L. Wu, C.-C.M. Ma, C.-H. Li, T.-M. Lee, C.-Y. Chen, C.-L. Chiang, C. Wu, *J. Membr. Sci.* 280 (2006) 501–508.
- [10] S.M.J. Zaidi, *Electrochim. Acta* 50 (2005) 4771–4777.
- [11] J.-W. Rhim, C.-K. Yeom, S.-W. Kim, *J. Appl. Polym. Sci.* 68 (1998) 1717–1723.
- [12] W.-Y. Chiang, C.-L. Chen, *Polymer* 39 (1998) 2227–2233.
- [13] J.-W. Rhim, Y.-K. Kim, *J. Appl. Polym. Sci.* 75 (2000) 1699–1707.
- [14] J.-W. Rhim, M.-Y. Sohn, H.-J. Joo, K.-H. Lee, *J. Appl. Polym. Sci.* 50 (1993) 679–684.
- [15] B.S. Pivovar, Y. Wang, E.L. Cussler, *J. Membr. Sci.* 154 (1999) 155–162.
- [16] L. Li, Y. Wang, *Chin. J. Chem. Eng.* 10 (2002) 614–617.
- [17] L. Li, L. Xu, Y. Wang, *Mater. Lett.* 57 (2003) 1406–1410.
- [18] W. Xu, C. Liu, X. Xue, Y. Su, Y. Lv, W. Xing, T. Lu, *Solid State Ionics* 171 (2004) 121–127.
- [19] M.-S. Kang, J.H. Kim, J. Won, S.-H. Moon, Y.S. Kang, *J. Membr. Sci.* 247 (2005) 127–135.
- [20] D.S. Kim, M.D. Guiver, S.Y. Nam, T.I. Yun, M.Y. Seo, S.J. Kim, H.S. Hwang, J.W. Rhim, *J. Membr. Sci.* 281 (2006) 156–162.
- [21] J. Qiao, T. Hamaya, T. Okada, *Chem. Mater.* 17 (2005) 2413–2421.
- [22] C.-S. Wu, F.-Y. Lin, C.-Y. Chen, P.P. Chu, *J. Power Sources* 160 (2006) 1204–1210.
- [23] J.-W. Rhim, H.B. Park, C.-S. Lee, J.-H. Jun, D.S. Kim, Y.M. Lee, *J. Membr. Sci.* 238 (2004) 143–151.
- [24] D.S. Kim, H.B. Park, J.W. Rhim, Y.M. Lee, *J. Membr. Sci.* 240 (2004) 37–48.
- [25] A.M. Kannan, A. Menghal, I.V. Barsukov, *Electrochem. Commun.* 8 (2006) 887–891.
- [26] H.S. Mansur, R.L. Oréfice, A.A.P. Mansur, *Polymer* 45 (2004) 7193–7202.
- [27] J. Chen, M. Asano, T. Yamaki, M. Yoshida, *J. Membr. Sci.* 256 (2005) 38–45.